Metalla-macro-tricyclic cryptands: anion encapsulation and selective separation of sulfate *via in situ* crystallization†‡

N. N. Adarsh,[a] Derek A. Tocher,[b] Joan Ribas[c] and Parthasarathi Dastidar*[a]

Received (in Gainesville, FL, USA) 12th October 2009, Accepted 18th June 2010
DOI: 10.1039/b9nj00556k

A conformationally flexible bis-pyridyl-bis-amide ligand, namely *N*,*N*′-bis-(3-pyridyl)-isophthalamide (**L1**), has been exploited to synthesize metalla-macro-tricyclic cryptands by reacting it with various Cu(II) salts having different counteranions. Out of the five coordination compounds, namely $[\{Cu(\mu\text{-}\mathbf{L1})_2(H_2O)_2\}\cdot SO_4\cdot 2H_2O\cdot X]$ (**1a**), $[\{Cu(\mu\text{-}\mathbf{L1})(H_2O)_4\}\cdot SO_4\cdot 3H_2O]_\infty$ (**1b**), $[\{Cu(\mu\text{-}\mathbf{L1})_2(H_2O)_2\}\cdot SiF_6\cdot CH_3OH\cdot 4H_2O]_\infty$ (**2**), $[\{Cu(\mu\text{-}\mathbf{L1})_2(\mu\text{-}Cl)\}\cdot ClO_4]_\infty$ (**3**) and $[\{Cu(\mu\text{-}\mathbf{L1})_2(H_2O)\}\cdot(NO_3)_2\cdot 2H_2O\cdot X]_\infty$ (**4a**) (X = disordered solvents), compounds such as **1a**, **2** and **3** are metallacryptands, of which **3** is the first example of a polymeric metalla-macro-tricyclic cryptand. The effect of the conformation-dependent ligating topology and hydrogen bonding backbone of ligand **L1**, and counteranions on the formation of metallacryptands is discussed. Interestingly, an important anion, namely SO_4^{2-}, has been separated by concomitantly crystallizing **1a** and **1b** from a complex mixture of anions, such as SO_4^{2-}, NO_3^- and ClO_4^-, by following an *in situ* crystallization technique. Magnetic interactions in **3** have been investigated as a typical example. Weak antiferromagnetic coupling is observed in **3**, as expected given the topology of the networks.

Introduction

The journey of anion encapsulation within a cryptand host started with the seminal work by Park and Simmons.[1] Cryptands suitable for cation encapsulation originally developed by Lehn[2] underwent an evolution process and a plethora of different types of cryptands emerged for anion encapsulation. For example, Bowman-James,[3] Ghosh,[4] Nelson[5] and others[6] have developed cryptands for anion encapsulation. These anion receptors are accessible only by non-trivial multi-step organic synthesis. Supramolecular synthesis, on the other hand, is an alternative approach, wherein non-covalent interactions play a major role in forming an assembly of molecules that displays intriguing supramolecular architectures and functions;[7] in particular, metal–ligand coordination has been exploited extensively for constructing various supramolecular architectures, such as interlocking rings,[8] linear and circular helicates,[9] and molecular cages and boxes,[10] triangles,[11] squares,[12] pentagons,[13] hexagons;[14] these topologies are otherwise difficult to obtain in an alternative stepwise covalent synthetic approach.

To further explore our interest in encapsulation and the selective separation of anions[23b,d] by metal–organic hosts, we have considered exploiting a supramolecular approach to synthesize and evaluate anion encapsulation and separation by metalla-macro-tricyclic cryptands of the kind depicted in Scheme 1. This may be considered as metalla-analogue of tricyclic organic cryptands,[15] and may be obtained by coordinating an N-donor bidentate ligand with an appropriate ligating topology to a suitable metal center.

Success in the synthesis of the metallacryptand lies in the ligating topology of the ligand, on the coordination geometry of the metal center and on the nature of the counteranions. Moreover, numerous secondary factors, such as the lack of control over the metal : ligand ratio,[16] solvents,[17] concentration,[18] counteranions[19] and temperature,[20] play crucial roles in the formation of the thermodynamically (or kinetically) favored end products, and therefore often make it difficult to predict the final outcome. Nevertheless, there are a number of reports pertaining to the synthesis and characterization of

Scheme 1

---

[a] Department of Organic Chemistry, Indian Association for the Cultivation of Science, 2A & 2B Raja S. C. Mullick Road, Kolkata 700032, India
[b] Department of Chemistry, University College London, 20 Gordon Street, London WC1H 0AJ, UK
[c] Departament de Química Inorgánica Universitat de Barcelona, Diagonal, 647, 08028-Barcelona, Spain.
E-mail: parthod123@rediffmail.com, ocpd@iacs.res.in

† This article is part of a themed issue on Coordination polymers: structure and function.

‡ Electronic supplementary information (ESI) available: Molecular plots and hydrogen bonding parameters for **1a–4a**, XRPD simulated-bulk comparison plot for **2**, **3** and **4a**, thermogravimetric plots (Fig. S1–S3), experimental details for anion binding studies, FT-IR data (Table S1), EPR spectra (Fig. S4), and crystallographic data. CCDC reference numbers 739005–739007, 739009 and 739010. For ESI and crystallographic data in CIF or other electronic format see DOI: 10.1039/b9nj00556k

metallacryptands of various kinds.[21] However, there are not many reports on metalla-macro-tricylic cryptands of the kind shown in Scheme 1.[22]

As a part of our ongoing research endeavour in synthesizing intriguing coordination polymers (CPs) and/or metal–organic frameworks (MOFs), we are interested in studying the effect of the hydrogen bonding backbone of the ligands, the conformation and positional isomerisation-dependent ligating topology of the ligands, and counteranions on the resultant MOF structures.[23]

In this article, we report a systematic study on the effect of counteranions, the conformation-dependent ligating topology and hydrogen bonding backbone of the ligand on the final supramolecular products in an attempt to synthesize Cu(II)-metallacryptands. When reacted with Cu(II) salts having various counteranions using an identical solvent system (aqueous EtOH–MeOH), a bis-pyridyl-bis-amide ligand, namely *N*,*N*′-bis-(3-pyridyl)isophthalamide (**L1**), resulted in two discrete metallacryptands $[\{(4H_2O)(2SO_4^{2-}) \subset Cu_2(\mathbf{L1})_4(H_2O)_4\}\cdot H_2O\cdot X]$ (**1a**) and $[(4H_2O)(2SiF_6) \subset \{Cu_2(\mathbf{L1})_4(H_2O)_4\}MeOH\cdot H_2O\cdot X]$ (**2**), a 1D coordination polymeric metallacryptand $[\{4ClO_4 \subset Cu_2(\mathbf{L1})_4(H_2O)_2(\mu\text{-}Cl)_2\}]_\infty$ (**3**) and a looped chain 1D coordination polymer $[\{Cu(\mu\text{-}\mathbf{L1})_4(H_2O)\}\cdot NO_3\cdot 2H_2O]_\infty$ (**4a**) (Scheme 2); a 1D zigzag coordination polymer $[\{Cu(\mu\text{-}\mathbf{L1})(H_2O)_4\}\cdot SO_4\cdot 3H_2O]_\infty$ (**1b**) was also isolated as occasionally occurring concomitant X-ray quality crystals while synthesizing **1a**. Based on the single crystal X-ray data, the role of the counteranions, hydrogen bonding backbone of the ligand and conformation-dependent ligating topology of the ligand **L1** on the resultant supramolecular structures of **1a–4a** is discussed. It has also been shown that sulfate anion can be separated from a complex mixture of various oxo-anions, such as sulfate, nitrate and perchlorate, in the form of **1a** (as neat crystals) and **1b** (as a microcrystalline powder) *via in situ* crystallization techniques. Magneto-structural correlations in MOFs have become important in recent years. However, such studies involving metallacryptands, wherein the magnetic properties are affected by the counteranions, have rarely been reported.[24] Thus, we also report here magnetic studies of the chloride-bridged 1D coordination polymer of metallacryptand **3**.

Results and discussion

Ligand **L1** has been exploited by Puddephatt's group to study various supramolecular structures,[25] including metallacryptands.[22e,g] We have also exploited ligand **L1** and its positional isomer, namely *N*,*N*′-bis-(4-pyridyl)isophthalamide, to study ligating topology and counterion-dependent supramolecular structural diversity, and intriguing anion separation from a complex mixture.[23b] In the present study, we decided to work with **L1** because it can adopt a suitable ligating topology, *i.e. anti-syn-anti*, conducive to metallacryptand formation (Scheme 2 and Scheme 3); the hydrogen bonding backbone, namely bis-amide moieties, are expected to trap counteranions/guest molecules within the metalla-cage *via* hydrogen bonding interactions. On the other hand, Cu(II) was chosen because it is quite flexible in terms of its coordination geometry (four, five or six coordinate), allowing a considerable amount

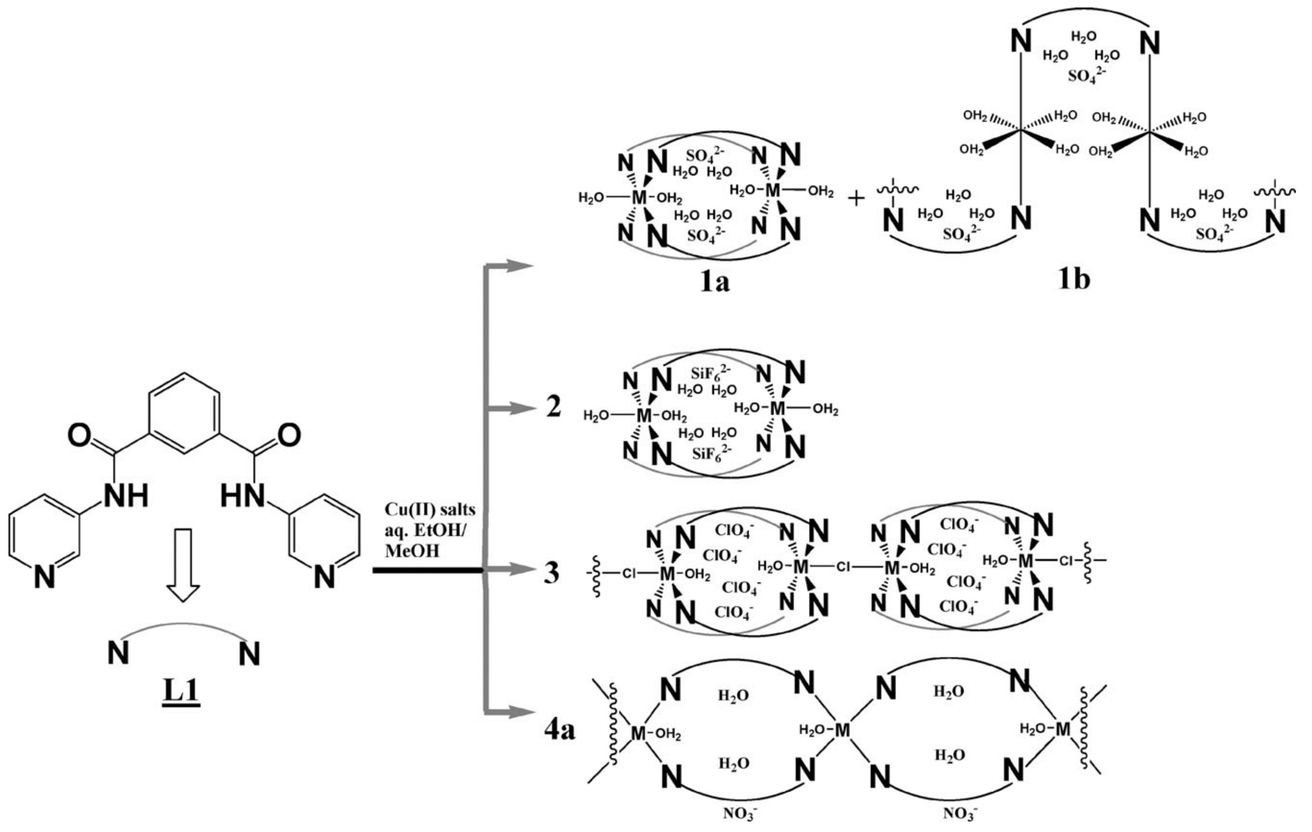

Scheme 2

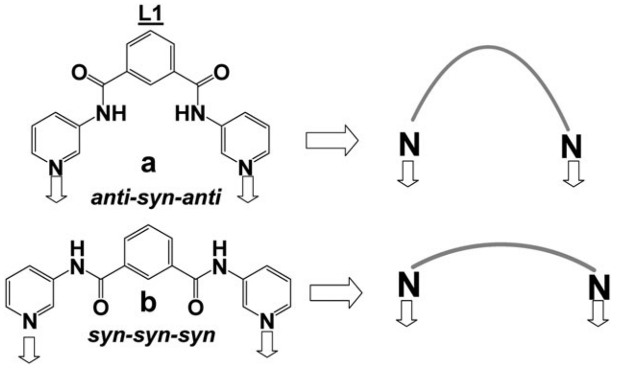

Scheme 3

of distortion to these geometries, associated with strains that may be built into the ligand itself during metallacryptand formation. Counteranions of various sizes and geometries, such as SO_4^{2-}, SiF_6^{2-}, ClO_4^- and NO_3^-, have been studied to observe the effect of counteranions on the supramolecular structures of the resultant compounds. The crystal data and selected bond distances and angles are recorded in Table 1 and Table 2, respectively.

Single crystal X-ray structures of the metallocryptands 1a, 2 and 3

Single crystal X-ray structural analyses reveal that compounds **1a**, **2** and **3** are all metallocryptands formed as a result of the coordination of the ligand *via* pyridyl N atoms to the Cu(II) metal center in a 1 : 2 (metal : ligand) ratio. Both **1a** and **2** are isomorphous metalla-macro-tricyclic cryptands displaying identical space groups (triclinic, $P\bar{1}$) and similar cell dimensions (Table 1). Pd(II) complexes of **L1**, which are isostructural with **1a** and **2**, have been reported by Puddephatt.[22e] Compound **3** was found to be the first example of a 1D coordination polymer of a metalla-macro-tricyclic cryptand, which crystallized in the centrosymmetric tetragonal space group $I4/m$. In this structure, Cl^-, Cu(II) and metal-bound water are all located on a 4-fold axis, whereas the ligands are positioned on a 2-fold axis. Surprisingly, the metallacryptand moieties are bridged by chloride. The chloride anion in this structure appears to have come from impurities in the water used for the synthesis. Well refined single crystal data of **3**, a nearly superimposable simulated X-ray powder diffraction (XRPD) pattern with that of the bulk crystals of **3** and accurate microanalysis data clearly support the presence of chloride as a bridging ligand in the structure of **3**. Metallacryptand **3** was also isolated in presence of dilute HCl. Thus, it appears that one of the ClO_4^- ions needed for charge balance has been exchanged by Cl^-, either present as an impurity or deliberately added (*vide infra*) (see the Experimental and ESI‡). Ligand **L1** displays a severely non-planar *anti-syn-anti* conformation (Scheme 3), as revealed by the dihedral angles involving the terminal pyridyl rings and the central aromatic ring

Table 1 Crystal data

Crystal parameter	1a	1b	2	3	4a
CCDC no.	739006	739010	739007	739005	739009
Empirical formula	$C_{72}H_{92}Cu_2N_{16}O_{34}S_2$	$C_{18}H_{28}CuN_4O_{13}S$	$C_{74}H_{88}Cu_2F_{12}N_{16}O_{22}Si_2$	$C_{72}H_{60}Cl_4Cu_2N_{16}O_{22}$	$C_{36}H_{35}CuN_{10}O_{13.50}$
Formula weight	1916.82	604.04	1964.86	1770.24	887.28
Crystal size/mm	0.30 × 0.20 × 0.06	0.24 × 0.18 × 0.08	0.21 × 0.11 × 0.08	0.12 × 0.12 × 0.10	0.20 × 0.12 × 0.08
Crystal system	Triclinic	Monoclinic	Triclinic	Tetragonal	Monoclinic
Space group	$P\bar{1}$	$P2_1/c$	$P\bar{1}$	$I4/m$	Cm
a/Å	12.874(3)	7.1978(4)	13.089(5)	15.7237(8)	13.3120(12)
b/Å	13.211(3)	16.6218(10)	13.512(5)	15.7237(8)	21.515(3)
c/Å	14.871(4)	20.5689(12)	14.983(9)	14.9552(16)	8.2165(10)
α (°)	103.703(3)	90.00	105.233(12)	90.00	90.00
β (°)	99.287(3)	96.2260(10)	97.716(12)	90.00	122.978(5)
γ (°)	112.473(3)	90.00	113.793(8)	90.00	90.00
Volume/Å^3	2179.4(9)	2446.4(2)	2251.1(17)	3697.4(5)	1974.1(4)
Z	1	4	1	2	2
D_{calc}/g cm^{-3}	1.460	1.640	1.449	1.590	1.492
F(000)	998	1252	1014	1812	916
$\mu_{Mo\text{-}K_\alpha}$/mm^{-1}	0.630	1.053	0.601	0.810	0.633
Flack parameter	Not applicable	Not applicable	Not applicable	Not applicable	0.498(16)[a]
T/K	100(2)	100(2)	100(2)	150(2)	100(2)
R_{int}	0.0471	0.0364	0.0687	0.0680	0.0601
Range of h, k, l	−12/12, −12/12, −14/14	−8/8, −19/19, −24/24	−12/12, −13/13, −14/14	−20/20, −20/20, −19/19	−15/17, −27/27, −10/10
$\theta_{min}/\theta_{max}$	1.47/20.00	1.58/27.24	1.46/20.58	1.88/28.26	1.89/27.48
Reflections collected/unique/observed [$I > 2\sigma(I)$]	12647/4062/3285	23124/4317/3653	14018/4545/3339	16240/2351/1896	7263/3602/3329
Data/restraints/parameters	4062/4/539	4317/0/390	4545/4/594	2351/0/181	3602/2/277
Goodness of fit on F^2	1.051	1.056	1.057	1.053	1.012
Final R indices [$I > 2\sigma(I)$]	R_1 = 0.0457 wR_2 = 0.1207	R_1 = 0.0273 wR_2 = 0.0738	R_1 = 0.0568 wR_2 = 0.1508	R_1 = 0.0658 wR_2 = 0.1639	R_1 = 0.0551 wR_2 = 0.1356
R indices (all data)	R_1 = 0.0577 wR_2 = 0.1288	R_1 = 0.0345 wR_2 = 0.0779	R_1 = 0.0795 wR_2 = 0.1660	R_1 = 0.0833 wR_2 = 0.1743	R_1 = 0.0585 wR_2 = 0.1382

[a] We used BASF and TWIN commands to refine Flack and obtained a value of 0.498(16), which could point to a 50 : 50 twin. It may be mentioned that we started refining the BASF parameter with 0.4 in order to avoid a pseudo-minimum BASF.

Table 2 Selected bond lengths and bond angles

1a			
Bond length	Bond length	Bond angle	Bond angle
Cu(1)–N(47)	2.021(4)	N(47)–Cu(1)–N(1)	90.22(17)
Cu(1)–N(1)	2.031(4)	N(23)–Cu(1)–N(25)	90.48(16)
Cu(1)–N(23)	2.008(4)	N(1)–Cu(1)–N(25)	89.86(16)
Cu(1)–N(25)	2.025(4)	N(23)–Cu(1)–N(47)	89.60(17)
Cu(1)–O(49)	2.427(4)	N(23)–Cu(1)–O(49)	94.48(16)
		N(47)–Cu(1)–O(49)	89.13(15)
		N(25)–Cu(1)–O(49)	88.95(15)
		N(1)–Cu(1)–O(49)	90.47(16)
1b			
Cu(1)–O(28)	2.0050(16)	O(26)–Cu(1)–O(27)	96.31(7)
Cu(1)–O(26)	1.9860(16)	O(26)–Cu(1)–N(23)	87.60(7)
Cu(1)–N(23)	2.0147(17)	O(28)–Cu(1)–N(23)	91.52(7)
Cu(1)–N(1)	2.0197(17)	O(26)–Cu(1)–N(1)	91.54(7)
Cu(1)–O(27)	2.3730(17)	O(28)–Cu(1)–N(1)	89.43(7)
Cu(1)–O(25)	2.4278(16)	O(28)–Cu(1)–O(27)	85.34(7)
		N(23)–Cu(1)–O(27)	86.60(6)
		N(1)–Cu(1)–O(27)	90.56(6)
		O(26)–Cu(1)–O(25)	84.76(7)
		O(28)–Cu(1)–O(25)	93.56(7)
		N(23)–Cu(1)–O(25)	91.92(6)
		N(1)–Cu(1)–O(25)	90.95(6)
2			
Cu(1)–N(1)	2.043(5)	N(1)–Cu(1)–N(25)	90.5(2)
Cu(1)–N(25)	2.022(5)	N(25)–Cu(1)–N(23)	90.3(2)
Cu(1)–N(23)	2.027(5)	N(1)–Cu(1)–N(47)	90.3(2)
Cu(1)–N(47)	2.015(6)	N(23)–Cu(1)–N(47)	89.0(2)
Cu(1)–O(49)	2.341(5)	N(1)–Cu(1)–O(49)	90.7(2)
		N(25)–Cu(1)–O(49)	88.5(2)
		N(23)–Cu(1)–O(49)	93.2(2)
		N(47)–Cu(1)–O(49)	90.0(2)
3			
Cu(1)–N(1)	2.025(3)	N(1)–Cu(1)–N(1)	89.999(1)
Cu(1)–Cl(1)	2.8817(9)	N(1)–Cu(1)–O(2)	89.78(9)
Cu(1)–O(2)	2.478(6)	N(1)–Cu(1)–Cl(1)	90.22(9)
4a			
Cu(1)–N(1)	2.028(4)	N(1)–Cu(1)–N(1)	88.2(2)
Cu(1)–N(23)	2.032(3)	N(1)–Cu(1)–N(23)	87.77(12)
Cu(1)–O(25)	2.267(4)	N(23)–Cu(1)–N(23)	94.12(19)
		N(1)–Cu(1)–O(25)	97.01(12)
		N(23)–Cu(1)–O(25)	94.06(12)

(62–64 and 30–57° in **1a**, 64–66° and 31–55° in **2**, and 49° in **3**). It may be noted that **L1**, being highly flexible due to the free rotation of N_{amide}–$C_{pyridyl}$ bond, displays various conformations in the reported structures;[22e,25g] among them, *syn-anti-anti* was found to be the most frequent. While the hydrogen bond acceptor amide carbonyls all protrude out of the metallcryptands, the hydrogen bond donor amide N–H bonds are all disposed inside the metallcryptands in the structures of **1a**, **2** and **3**, resulting in interesting anion and other guest recognition inside the cage. The Cu(II) metal center in these structures adopts a six-coordinate slightly distorted octahedral geometry (see Table 2), resulting in partial occupation of the cage space by metal-bound water molecules.

Thus, in **1a** the cage is filled with two sulfate counteranions, four guest water molecules and two metal-bound water molecules, displaying various hydrogen bonding interactions among themselves, as well as with the amide N–H; each sulfate is hydrogen bonded to the amide N–H [N···O = 2.768(5)–2.780(5) Å; ∠ N–H···O = 153.1–157.6°], the metal-bound water [O···O = 2.765(6)–2.803(6) Å; ∠ O–H···O = 162(5)–164(6)°] and two guest water [O···O = 2.656(6)–2.781(6) Å] molecules, which were found to be a hydrogen bonded dimer [O···O = 2.733(6) Å]. One of the guest water molecules also forms hydrogen bonding interactions with the amide N–H of the ligand molecule [N···O = 2.918(5)–2.955(5) Å; ∠N–H···O = 165.8–170.7°] (Fig. 1a).

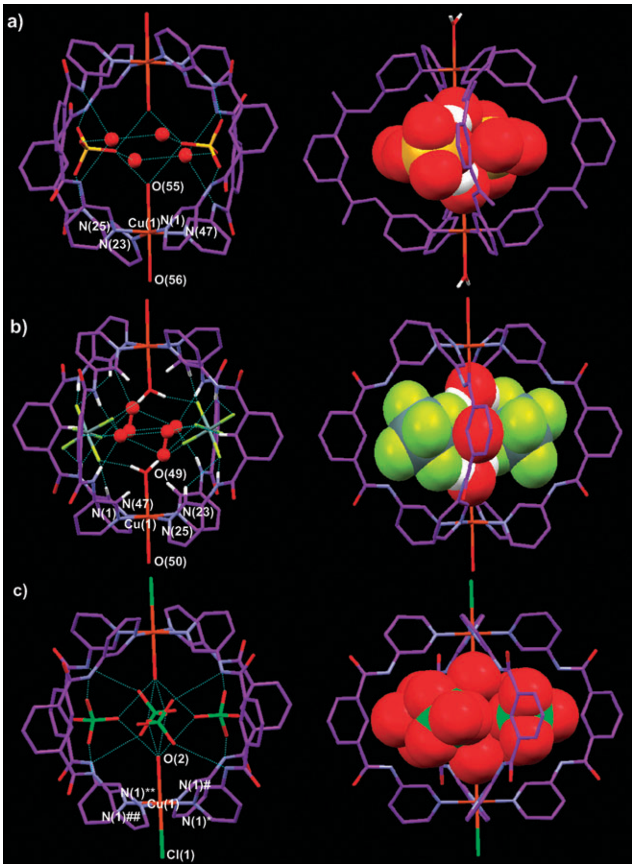

Fig. 1 Crystal structure illustration of (a) **1a**, (b) **2** and (c) **3**; anions are shown in a space-filling model in the right-most part of the figure to depict the encapsulated nature of the anions within the metallacryptand cage (symmetry code: * = 1 − *x*, 1 − *y*, 1 − *z*; ** = *x*, *y*, 1 − *z*; # = *y*, 1 − *x*, 1 − *z*; ## = 1 − *y*, *x*, 1 − *z*).

The cage of **2**, on the other hand, is filled with two SiF_6^{2-} anions, four guest water molecules and two metal-bound water molecules. Two of the guest water molecules were found to be disordered over two positions with site occupancy factors (SOFs) of 0.64 and 0.36. Each SiF_6^{2-} anion was held in the cage *via* hydrogen bonding interactions with amide N–H [N···F = 2.831(7)–3.104(7) Å; ∠N–H···F = 142.9–157.9°], disordered guest water [O···F = 2.576(15)–2.82(2) Å] and metal-bound water [O···F = 2.656(7)–2.739(7) Å; ∠ O–H···F = 155(7)–173(7)°]. The ordered guest water molecules were found to be hydrogen bonded with the amide N–H [N···O = 2.961(8)–2.969(8) Å; ∠N–H···O = 167.8–174.7°] and disordered water molecule [O···O = 2.576(15)–2.624(18) Å] (Fig. 1b).

Interestingly, in **3**, no guest molecule was detected; instead, the cage is filled with four ClO_4^- counteranions having a 0.75 SOF that are curiously disordered over the 4-fold axis and two metal-bound water molecules. The counteranion ClO_4^- is held in the cage *via* hydrogen bonding interactions involving amide N–H [N···O = 3.030(7) Å; ∠ N–H···O = 148(5)°] and metal-bound water molecules [O···O = 2.978(8) Å; ∠ O–H···O = 175(15)°] (Fig. 1c).

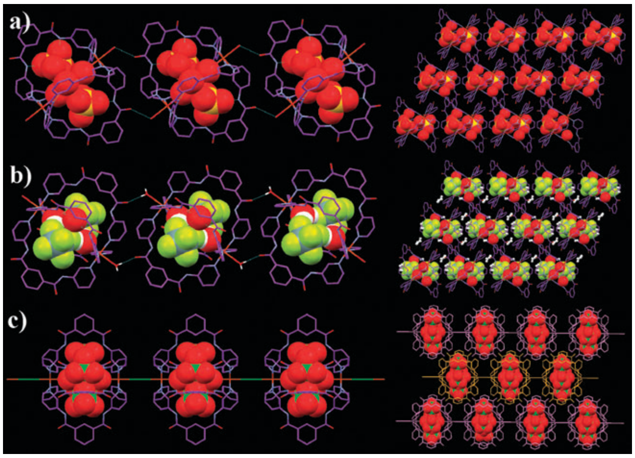

Fig. 2 Crystal structure illustrations; hierarchical self-assembly of the discrete metallacryptand cages *via* O–H···O interactions and their packing in (a) **1a** and (b) **2**; (c) 1D polymeric metallacryptand bridged *via* chloride and its crystal packing in **3**.

The hierarchical self-assembly of metallacryptands **1a** and **2** resulted in 1D hydrogen bonded chain, wherein the neighboring cages are held together *via* O–H···O hydrogen bonding [O···O = 2.768(5) and 2.775(7) Å; ∠ O–H···O = 170(5) and 171(8)° in **1a** and **2**, respectively] interactions involving amide carbonyl and metal-bound water. Such chains were packed in a parallel fashion and further stabilized by O–H···O interactions [O···O = 2.822(5) and 2.727(15)−2.82(2) Å in **1a** and **2**, respectively] involving amide carbonyl and a guest water molecule of the neighboring chain. A short contact involving amide carbonyl and amide N [O···N = 2.926(6) and 3.024(10) Å in **1a** and **2**, respectively] indicates the existence of >C=O···π interactions[26] in these two structures (Fig. 2a and b).

The metallacryptands in **3** are bridged by chloride *via* axial coordination to the metal centers of the adjacent metalla-cages, resulting in the formation of a 1D coordination polymer of metallacryptands (Fig. 2c). Interestingly, **3** is the first example of a 1D polymeric metalla-macro-tricyclic cryptand. Such 1D chains are packed in a parallel fashion and further stabilized by various non-bonding interactions, such as π···π [3.201(4)–3.385(7) Å] and C–H···O [C···O = 3.244(8)–3.498(10) Å; ∠C–H···O = 137(4)–160(6)°].

While refining the structures of **1a** and **2**, disordered electron densities located outside the cages were observed in the difference Fourier maps. No meaningful model could be built for the disordered electron densities in **1a**, whereas all the disordered electron density peaks in **2** could be modelled and refined (see the Experimental). Thus, in **2**, three disordered water molecules and one disordered MeOH were located outside the cage. SQUEEZE[27] was applied in **1a** to discard the contribution of the unmodelled disordered electron density peaks. 95.6 e unit cell^{-1} and a 411.5 Å^3 solvent accessible area volume were found in **1a** by SQUEEZE calculations. Thus, ~50 e asymmetric unit^{-1} in **1a** may be attributed to five water molecules, resulting in a total of nine water (2 metal-bound, 2 located and 5 disordered guest water molecules revealed by SQUEEZE) molecules. However, thermogravimetric (TG) data of **1a** indicated a weight loss of 6.9% within the temperature range 26–226° C, which could be attributed to 4 water molecules (2 metal-bound and 2 guest already located in the crystal structure; calcd. weight loss for nine water molecules = 17%) (Fig. S1‡). It appears that the five loosely bound disordered water molecules, as revealed by SQUEEZE, were desolvated before loading the sample for TG experiments.

On the other hand, a weight loss of 15.6% within the temperature range 30–260° C in TG data of **2** corroborate well with the single crystal data (calc. weight loss for six water molecules + 1 MeOH = 14.3%) (Fig. S2‡).

X-Ray single crystal structures of the coordination polymers 1b and 4a

Coordination polymer **1b**—the occasionally occurring concomitant product appearing as pale blue X-ray quality crystals while synthesizing **1a**—was found to be a 1D zig-zag coordination polymer resulting from the extended coordination of **L1** with the adjacent Cu(II) metal center in a 1 : 1 metal : ligand ratio. Thus, the concomitant formation of **1b** with **1a** clearly emphasizes the dynamic nature of metal–ligand coordination bonding that results from the lack of control over the metal : ligand ratio in such supramolecular syntheses of metal–organic compounds. Thus, the 1 : 2 metal : ligand ratio in **1a** dictated the formation of a discrete metallacryptand, whereas the 1 : 1 metal : ligand ratio in **1b** is the reason for the formation of a 1D zig-zag coordination polymeric chain. The organic linker **L1** in **1b** displays the same *anti-syn-anti* (a, Scheme 2) conformation as observed in **1a** with significant non-planarity, as evident from the dihedral angle of 20–26° involving the pyridyl moieties and the central aromatic ring. The metal center displays a slightly distorted octahedral geometry (Table 2), wherein the equatorial positions are occupied by four water molecules and the apical positions are coordinated by pyridyl N atoms of the adjacent ligands in a polymeric fashion, resulting in a 1D zig-zag coordination network (Fig. 3a). The 1D chains are further packed in parallel fashion, resulting in a channel type of open framework structure, wherein the channel space is occupied by the sulfate counteranions and guest water molecules (Fig. 3b). Interestingly, the amide N atoms abstain from any hydrogen bonding interactions, whereas the amide carbonyl O atoms are found to be involved in hydrogen bonding with the guest [O···O = 2.743(2) Å; ∠ O–H···O = 169(3)°] and the metal-bound [O···O = 2.783(2) Å; ∠ O–H···O = 179(3)°] water molecules of the neighboring polymeric chain. The sulfate counteranion and three guest water molecules are located in the channel space *via* various hydrogen bonding interactions; the sulfate forms various hydrogen bonding contacts with the guest [O···O = 2.652(2)–2.722(2) and 2.651(2)–2.770(3) Å; ∠O–H···O = 168(3)–171(3)°] as well as the metal-bound [O···O = 2.701(2)–2.726(2) Å; ∠O–H···O = 169(2)–176(3)°] water molecules; the guest water molecules were found to form a hydrogen bonded trimer [O···O = 2.781(3)–2.806(3) Å; ∠O–H···O = 170(3)–174(3)°]. Such interactions lead to the formation of a 1D hydrogen bonded chain of sulfate–water clusters that run through the channel (Fig. 3c).

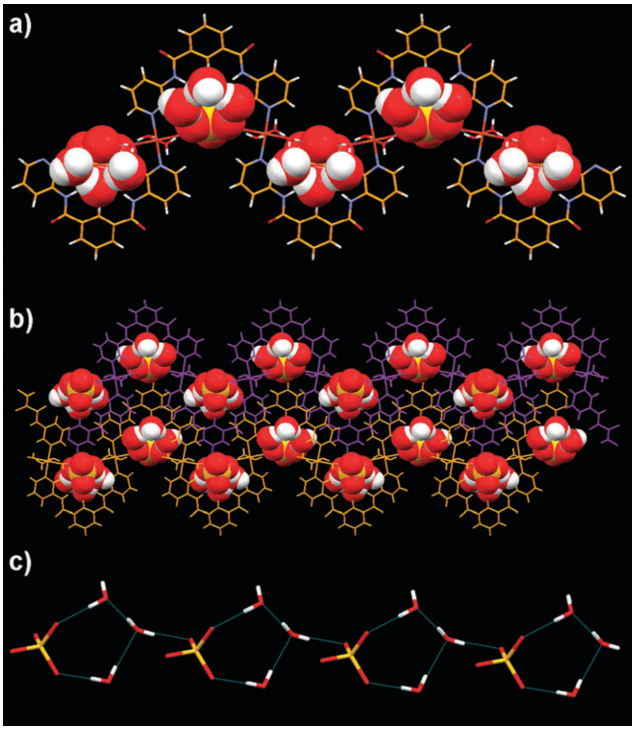

Fig. 3 A crystal structure illustration of **1b**; (a) 1D zig-zag coordination polymer; (b) parallel packing of the 1D zig-zag coordination polymer displaying a channel-type architecture encapsulating sulfate and guest water molecules (shown in a space filling model); (c) the sulfate–water hydrogen bonded cluster that runs through the channel space.

The *syn-syn-syn* conformation (b in Scheme 3) of **L1** and the 1 : 2 metal : ligand ratio resulted in a 1D coordination polymer with a looped chain topology in **4a**. Organic linker **L1** in the structure displays a non-planar conformation with dihedral angles of 38–54° involving the pyridyl moieties and the central aromatic ring. The metal center in **4a** displays a slightly distorted square pyramidal geometry (Table 2), wherein the equatorial positions are occupied by pyridyl N atoms of the ligand molecules and the apical position is coordinated by a water molecule. In this structure, extended coordination of the organic linker with the metal center results in the formation of a 1D looped chain coordination polymer having a staircase-like architecture. These chains are held together in a parallel fashion *via* N–H···O hydrogen bonding, involving the counter-anion nitrate [N···O = 2.801(4)–2.870(4) Å; ∠N–H···O = 145.4–154.3°]. The guest water molecules are trapped within the interstitial space, and held *via* hydrogen bonding interactions involving the amide carbonyl O atoms and the metal-coordinated water molecules of adjacent chains [O···O = 2.690(7)–2.727(8) Å] (Fig. 4).

SQUEEZE calculations revealed the presence of 54 e unit cell^{-1} with a 224.2 Å^3 solvent accessible area volume in **4a**, which may be attributed to three water molecules. As a result, a total of six water molecules (two guest, one metal-bound and three disordered water molecules, as obtained with SQUEEZE) are seen in the crystal structure of **4a**. TG data showed a weight loss of 7.5% within the temperature range 29–138° C, which does not match well with the single crystal X-ray data (calcd. weight loss for six water molecules = 11.6%) (Fig. S3‡). This could be because of the loss of some of the disordered water molecules before TG experiments were performed.

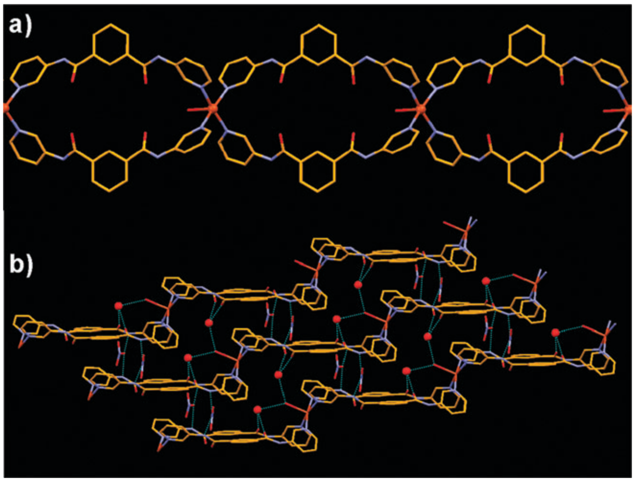

Fig. 4 Crystal structure illustration of **4a**; (a) 1D looped chain coordination polymer; (b) parallel packing of the 1D chains *via* various hydrogen bonding (shown as dotted lines).

Separation of sulfate anions *via* an *in situ* crystallization techniques

One of the important aspects of CPs and/or MOFs is their ability to exchange anions.[28] Since the first example of anion exchange in a MOF,[29] it was quickly realized that these metal–organic systems can be exploited to recognize and separate important anions.[23b,d,30] The widely accepted view of the anion exchange mechanism in CPs and/or MOFs is solid state mediated anion exchange, wherein the framework retains its structural integrity, as in the cases of ion-exchange resins or zeolites. However, this kind of exchange pathway was recently challenged; it has been shown that, in at least some 1D CPs, the mechanism involves dissolution and re-crystallization of the corresponding CP crystals.[31] Thus, *in situ* crystallization of CPs has been proposed to be an alternative method to separate a targeted anion from a complex mixture of anions,[28] wherein the organic linker and metal salts having various counter-anions are allowed to crystallize together. Since the separation of sulfate is important,[32] a systematic study of *in situ* crystallization experiments under non-competitive and competitive conditions was undertaken in order to separate sulfate anions from a complex mixture of anions (Scheme 4).

It is clear from Scheme 4 that the observation remained the same in each set of conditions (Fig. 5). Both the crystals (A, C, E and G) and the powder (B, D, F and H) were characterized by X-ray powder diffraction (XRPD), FT-IR, elemental analysis and energy dispersive X-ray spectroscopy (EDX).

Fig. 6 depicts the FT-IR spectra of the crystals obtained under various conditions. It reveals that the chemical nature of the compounds isolated under various conditions must be similar to that of **1a**, whereas their crystalline phase purity could not be determined since XRPD patterns recorded on the crystals harvested under various conditions did not match

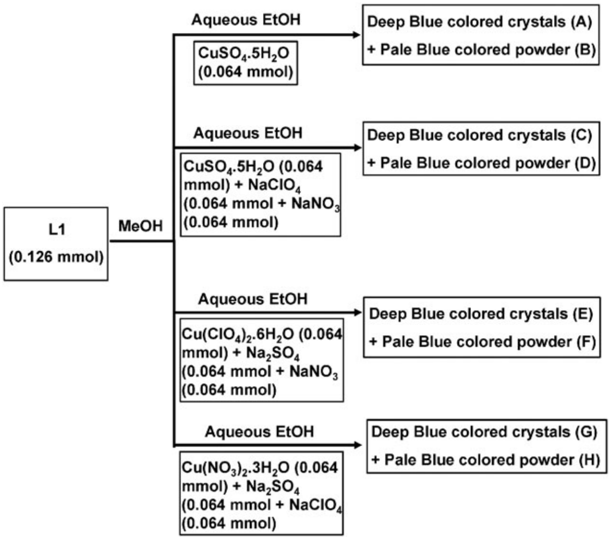

Scheme 4

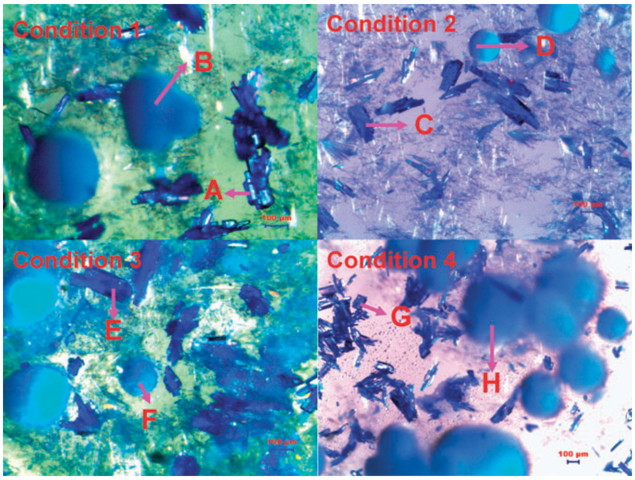

Fig. 5 Optical micrographs of the experiments depicted in Scheme 4.

with the simulated pattern of **1a** (patterns not shown), presumably due to the rapid loss of the lattice-included solvents.

Fig. 7, on the other hand, depicts FT-IR spectra of the pale blue colored powder obtained under various conditions. These data indicate that the bulk pale blue powder obtained in condition 1, which is non-competitive in nature, appears to comprise microcrystals of 1D zig-zag coordination polymer **1b**, since the IR spectrum of **1b** crystals and the bulk powder of condition 1 are nearly superimposable. The slight shift of the peaks near to 1200 cm^{-1} and the appearance of strong peaks around 1000 cm^{-1} may be due to the presence of a different supramolecular environment, which might occur as a result of the formation of various other crystalline forms of **1b** in the bulk under these competitive conditions (*i.e.* 2, 3 and 4). However, because of the corresponding XRPD patterns being weak and inconsistent, presumably due to the solvent loss during diffraction experiments, it is difficult to conclude with certainty on the crystalline phase purity of the bulk powder obtained under the various conditions (*i.e.* 1, 2, 3 and 4).

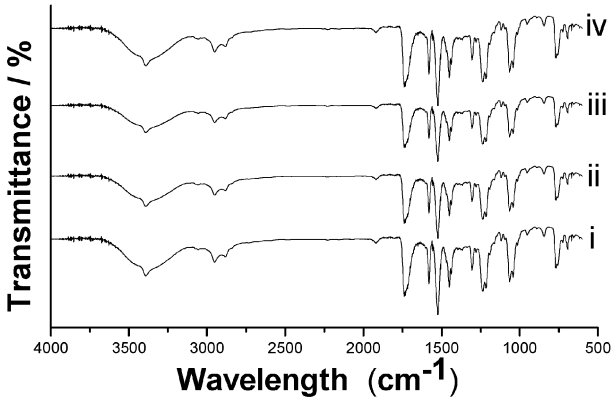

Fig. 6 FT-IR spectra of the deep blue colored crystals obtained under various conditions as depicted in Scheme 4; conditions 1, 2, 3 and 4 are shown in i, ii, iii and iv, respectively.

Nevertheless, elemental analysis results (Table 3) support the presence of coordination compound **1b**. Interestingly, the presence of a strong band in the range of 1103–1116 cm^{-1} in the FT-IR spectra of all the samples (A–H) clearly indicates the presence of ν_{asymm} S–O of the sulfate anion (Table S1‡). It can be seen that the deep blue crystals and the pale blue powder obtained under the various conditions are the metallacryptand **1a** and the 1D zig-zag CP **1b**, both having a different stoichiometry of lattice-included water, respectively.

EDX data collected on both the crystals and the powder samples supported the presence of all the elements expected from the corresponding coordination compounds having sulfate as counteranion (Fig. 8). It is important to note here that sulfate anion comes early in the Hofmeister series[33] which most often refers to the order of anions in the order of decreasing anion hydration energy or charge density. Thus, it is generally difficult to separate anion in *anti* Hofmeister fashion. However, in the present study, the separation of sulfate from a complex mixture of sulfate, nitrate and perchlorate of which both nitrate and perchlorate appear much later in the Hofmeister series due to their lower

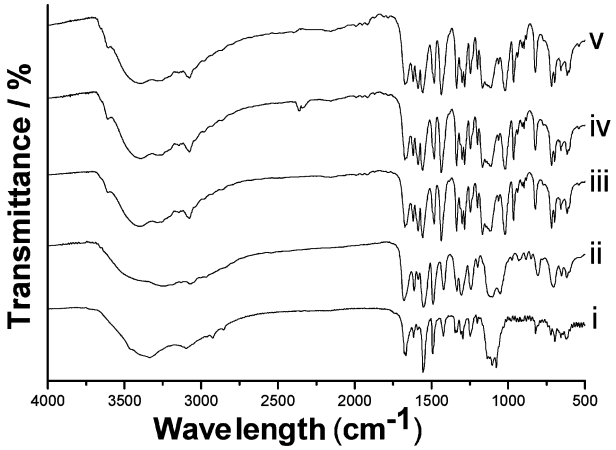

Fig. 7 FT-IR spectra of the pale blue colored powder obtained under various conditions, as depicted in Scheme 4; condition 1, 2, 3 and 4 are shown in ii, iii, iv and v, respectively (the FT-IR spectrum of the occasionally harvested pale blue crystals of **1b** is shown in i).

Table 3 Elemental analysis data

Crystallization condition	Elemental analysis for deep blue colored crystals (%)	Elemental analysis for pale blue colored powder (%)	Elemental analysis for pale blue colored crystals (%)
Condition 1	For $C_{72}H_{64}N_{16}O_{20}Cu_2S_2{\cdot}4H_2O$ Calcd. C 49.80, H 4.18, N 12.90; Found: C 50.45, H 3.82, N 12.71.	For $C_{18}H_{22}N_4O_{10}CuS{\cdot}H_2O$ Calcd. C 38.06, H 4.26, N 9.86; Found: C 38.47, H 3.73, N 10.53.	For $C_{18}H_{22}N_4O_{10}CuS{\cdot}3H_2O$ Calcd. C 35.79, H 4.67, N 9.28; Found: C 35.88, H 4.33, N 9.28.
Condition 2	For $C_{72}H_{64}N_{16}O_{20}Cu_2S_2{\cdot}6H_2O$ Calcd. C 48.78, H 4.32, N 12.64; Found: C 48.90, H 3.91, N 12.30.	for $C_{18}H_{22}N_4O_{10}CuS{\cdot}H_2O$ Calcd. C 38.06, H 4.26, N 9.86; Found: C 37.99, H 4.35, N 9.64.	
Condition 3	For $C_{72}H_{64}N_{16}O_{20}Cu_2S_2$. $6H_2O$ Calcd. C 48.78, H 4.32, N 12.64; Found: C 48.96, H 4.12, N 12.31.	For $C_{18}H_{22}N_4O_{10}CuS{\cdot}H_2O$ Calcd. C 38.06, H 4.26, N 9.86; Found: C 38.17, H 3.89, N 9.67.	
Condition 4	For $C_{72}H_{64}N_{16}O_{20}Cu_2S_2$. $6H_2O$ Calcd. C 48.78, H 4.32, N 12.64; Found: C 48.83, H 3.96, N 12.94.	For $C_{18}H_{22}N_4O_{10}CuS{\cdot}H_2O$ Calcd. C 38.06, H 4.26, N 9.86; Found: C 38.36, H 3.63, N 9.60.	

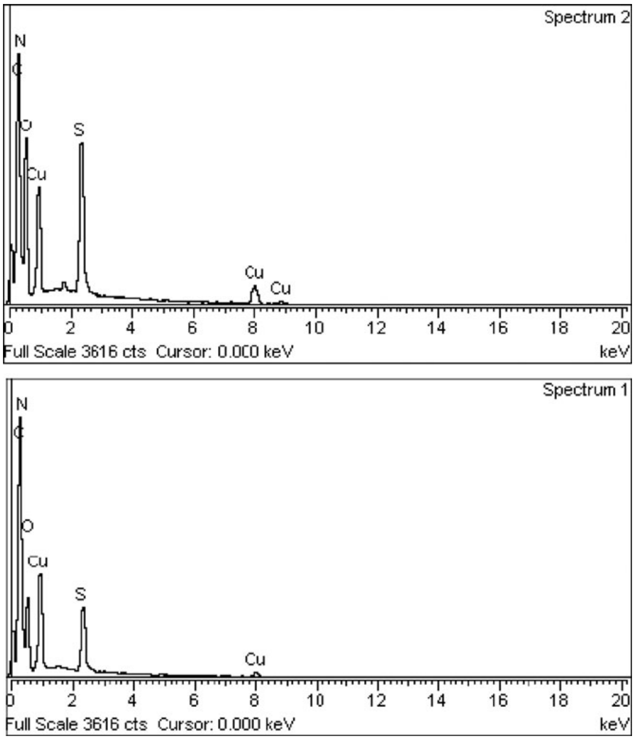

Fig. 8 EDX of deep blue colored crystals (top) and pale blue colored powder (bottom) obtained in condition 3; similar EDX results were obtained in other conditions.

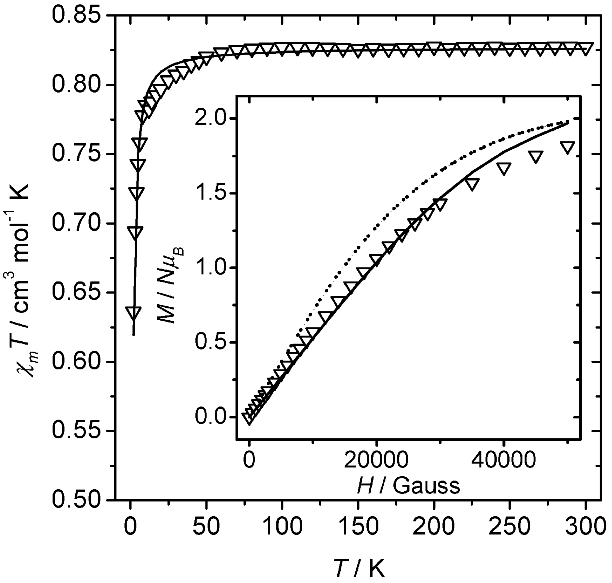

Fig. 9 Plot of $\chi_m T$ *vs.* T for complex **3**. Inset: plot of the reduced magnetization at 2 K. Solid lines represent the best fit for the two curves. The dotted curve in the inset is the plot of the Brillouin function for two independent copper(II) ions with g = 2.10.

hydration energy compared to that of sulfate is an example of anion selectivity that violates Hofmeister bias in this *in situ* crystallization of coordination compound. Unfortunately, when the competitive experiments were carried out in presence anions (nitrate and perchlorate taken in two times in excess compared to sulfate), no selectivity was observed. Thus, concentration of the anions plays a major role in such selectivity in the present system.

Magnetic studies. From the crystal structure, compound **3** can be considered as a 1D network, in which copper(II) ions are linked in an alternating form by the large ligand **L1** and by μ-Cl bridges at 2.88 Å (Cu–Cl). From this structural feature, we can deduce that these two magnetic pathways will be very close to zero, *i.e.* negligible. Indeed, the magnetic properties of complex **3** as a $\chi_M T$ *vs.* T plot (χ_M is the molar magnetic susceptibility for two Cu^{II} ions) and the reduced magnetization ($M/N\mu_B$ *vs.* H) are shown in Fig. 9. The value of $\chi_M T$ at 300 K is 0.82 cm^3 mol^{-1} K which, is as expected for two magnetically quasi-isolated spin doublets ($g > 2.00$). Starting from room temperature $\chi_m T$ values are practically constant to 50 K, and below 50 K they decrease quickly to 0.63 cm^3 mol^{-1} K at 2 K. This feature is characteristic of very weak antiferromagnetic interactions. The reduced molar magnetization at 2 K (Fig. 9, inset) clearly corroborates that the antiferromagnetic coupling is very small. The $M/N\beta$ value at 5 T is close to 1.8 $N\mu_B$ but the curve does not follow the Brillouin law. Before trying to fit these data, we obtained an EPR spectrum at room temperature to gain a clear idea of the best g values (Fig. S4‡); g values being $g_\parallel$ = 2.17 and $g_\perp$ = 2.06 (g_{average} is thus = 2.10). With this g_{average}, we can conclude that $\chi_m T$ at room temperature must be 0.826 cm^3 mol^{-1} K. We then used the TIP value necessary for each copper(II) to obtain this $\chi_m T$ value at room temperature. The fit of the susceptibility data was carried out simply assuming a dinuclear entity and applying the Bleaney–Bowers formula.[34] The best fit parameters obtained were $J = -1.2 \pm 0.1$ cm^{-1}, $g = 2.10 \pm 0.01$ and $R = 3.7 \times 10^{-5}$. Very similar J and g values were obtained by a full-diagonalization method from the curve of the magnetization at 2 K (Fig. 9, inset). In this case, the best fit parameters obtained were $J = -1.5 \pm 0.1$ cm^{-1}, $g = 2.10 \pm 0.01$ and $R = 2.1 \times 10^{-4}$. Thus, the two methods give almost identical results. It is important to emphasize that the $M/N\mu_B$ curve does not follow the Brillouin function for two isolated $S = 1/2$ spins (Fig. 9, inset), thus indicating weak antiferromagnetic interactions.

Conclusions

The role of the hydrogen bonding backbone, ligating topology of the ligand and counteranions in the formation of metallacryptands has thus been systematically studied. The conformationally-flexible ligand **L1** adopts an *anti-syn-anti* conformation that is favorable for metallacryptand formation only when the counteranions are SO_4^{2-}, SiF_6^{2-} and ClO_4^- (**1a**, **2** and **3**, respectively); whereas in the case of NO_3^-, ligand **L1** displays variations of the *syn-syn-syn* conformation (Scheme 3) to give a looped chain coordination polymer (**4a**). The 3D shape (tetrahedral and octahedral) and hydrogen bonding interactions of the counteranions (SO_4^{2-}, SiF_6^{2-} and ClO_4^-) with the amide backbone of the ligand appear to be an important factor in stabilizing the metallacryptand structures. Thus, these 3D counteranions might have served as templates for metallacryptand formation, like in cases where counter-anions act as templates for the synthesis of various metallacages.[35] In **4a**, the NO_3^- anion, being 2D (planar trigonal), might not have interacted favorably with the ligand hydrogen bonding bis-amide backbone to facilitate metallacryptand formation. The concomitant formation of 1D zig-zag coordination polymer **1b** along with the metallacryptand **1a**, and the unknown crystalline product **4b** along with 1D looped chain coordination polymer **4a** clearly indicates the complexity involved in synthesizing a desired metallacryptand. The *in situ* crystallization technique proved to be viable for separating an important anion, SO_4^{2-}, from a complex mixture of anions containing SO_4^{2-}, NO_3^- and ClO_4^-, wherein both **1a** and **1b** were crystallized out. These results clearly display an example of sulfate selectivity in an anti-Hofmeister fashion. Magnetic coupling in complex **3**, as an example, is almost negligible.

Experimental section

Materials and methods

All chemicals were commercially available (Aldrich) and used without further purification. Ligand *N*,*N*′-bis-(3-pyridyl)-isophthalamide **L1** was synthesized by following a reported procedure.[25b] The elemental analysis was carried out using a Perkin-Elmer 2400 Series-II CHN analyzer. TG analyses were performed on a SDT Q Series 600 Universal VA.2E TA instrument. X-Ray powder diffraction (XRPD) patterns were recorded on a Bruker AXS D8 Advance Powder (Cu-K$_{\alpha1}$ radiation, λ = 1.5406 Å) X-ray diffractometer. FT-IR spectra were recorded using Perkin-Elmer Spectrum GX and EDX was performed on a JSM 6700F instrument (JEOL, Japan).

Safety note

Perchlorate compounds are potentially explosive. Although no problem was encountered in the present study, care must be exercised when handling such compounds.

Syntheses of 1a–4a

[{Cu(μ-L1)$_2$(H$_2$O)$_2$}·SO$_4$·2H$_2$O·X] (1a) and [{Cu(μ-L1)(H$_2$O)$_4$}·SO$_4$·3H$_2$O]$_\infty$ (1b) (X = disordered solvent of crystallization). **1a** and **1b** were crystallized together as deep blue and pale blue colored block-shaped crystals, respectively, by layering a methanolic solution of **L1** (50 mg, 0.158 mmol) over an aqueous ethanolic solution of $CuSO_4{\cdot}5H_2O$ (19.72 mg, 0.079 mmol). Deep blue colored crystals of **1a** were obtained after 1 d (yield = 20 mg, 15%). Only a few crystals of **1b** were isolated (occasionally) after 1 week.

1a: for $C_{72}H_{64}N_{16}O_{20}Cu_2S_2{\cdot}4H_2O$ (%): Elemental analysis calcd. C 49.80, H 4.18, N 12.90; found: C 50.45, H 3.82, N 12.71. IR (KBr pellet): 3248 (m, water ν O–H), 3188 (w, amide ν N–H), 3076 (m, aromatic ν C–H), 1674 (s, amide ν C═O), 1614 (s, amide δ N–H), 1587m, 1552s, 1489s, 1421s, 1334s, 1300s, 1244s, 1197s, 1101 (s, SO_4^{2-} ν S–O), 1076m, 918m, 804m, 700m, 651m, 617m, 538w cm^{-1}.

1b: Elemental analysis calcd. for $C_{18}H_{22}N_4O_{10}CuS{\cdot}3H_2O$ (%): C 35.79, H 4.67, N 9.28; found: C 35.88, H 4.33, N 9.28. IR (KBr pellet): 3334 (m, water ν O–H), 3097 (m, amide ν N–H), 2925 (m, aromatic ν C–H), 2856w, 1670 (s, amide ν C═O), 1616 (s, amide δ N–H), 1587m, 1550s, 1488s, 1423s, 1338s, 1299s, 1245s, 1130s, 1103 (s, SO_4^{2-} ν S–O), 1078s, 983w, 817m, 721m, 696m, 653m, 619m, 524w cm^{-1}.

[{Cu(μ-L1)$_2$(H$_2$O)$_2$}·SiF$_6$·CH$_3$OH·4H$_2$O] (2). Coordination complex **2** was synthesized by layering a methanolic solution of **L1** (50 mg, 0.158 mmol) over an aqueous ethanolic solution of a mixture of $Cu(BF_4)_2$ (18.73 mg, 0.079 mmol) and $(NH_4)_2SiF_6$ (14 mg, 0.079 mmol). Blue colored crystals of **2** were obtained after 1 week (yield = 40 mg, 29%). Elemental analysis calcd. for $C_{72}H_{64}N_{16}O_{12}Cu_2Si_2F_{12}$ (%): C 49.23, H 3.67, N 12.76; found: C 49.62, H 3.86, N 12.92. IR (KBr pellet): 3437 (m, water ν O–H), 3294 (m, amide ν N–H), 3132w, 3088 (m, aromatic ν C–H), 1678 (s, amide ν C═O), 1612 (s, amide δ N–H), 1587m, 1548s, 1491s, 1421s, 1336s, 1301s, 1242s, 1197m, 1136m, 1111m, 1074w, 1062w, 1030w, 999w, 923w, 885w, 848w, 813s, 742sb, 723 (sb, SiF_6^{2-} ν Si–F), 702sb, 651w, 480w, 424w cm^{-1}.

[{Cu(μ-L1)$_2$(μ-Cl)}·ClO$_4$]$_\infty$ (3). Coordination polymer **3** was synthesized by layering a 10 ml methanolic solution of **L1** (50 mg, 0.158 mmol) over an aqueous ethanolic solution (8 ml) of $Cu(ClO_4)_2{\cdot}6H_2O$ (29.3 mg, 0.079 mmol) containing 0.5 M HCl (2 ml). Blue colored truncated octahedron-shaped crystals of **3** were obtained within a few days (yield = 60 mg, 43%). Elemental analysis calcd. for $C_{72}H_{60}N_{16}O_{22}Cl_4Cu_2$ (%): C 48.85, H 3.42, N 12.66; found: C 48.57, H 3.42, N 12.29. IR (KBr pellet): 3479 (sb, water ν O–H), 3369 (s, amide ν N–H), 3091 (m, aromatic ν C–H), 3074m, 3045m, 1687 (s, amide ν C═O), 1647w, 1610 (s, amide δ N–H), 1585m, 1541s, 1489s, 1415s, 1336s, 1307s, 1236s, 1197s, 1091 (sb, ClO_4^- ν Cl–O), 927m, 881m, 850m, 808s, 796s, 731s, 700s, 655m, 623s, 590m, 534m cm^{-1}.

[{Cu(μ-L1)$_2$(H$_2$O)}·(NO$_3$)$_2$·2H$_2$O·X]$_\infty$ (4a) and [{Cu(μ-L1)$_2$(H$_2$O)$_2$}·(NO$_3$)$_2$] (4b) (X = disordered solvent of crystallization). **4a** and **4b** were isolated as concomitant violet and blue colored block-shaped crystals, respectively, after 1 week by layering a methanolic solution of **L1** (50 mg, 0.158 mmol) over an aqueous ethanolic solution of $Cu(NO_3)_2\cdot 3H_2O$ (19 mg, 0.079 mmol).

4a: yield = 30 mg, 43%. Elemental analysis calcd. for $C_{36}H_{30}N_{10}O_{11}Cu\cdot 2H_2O$ (%): C 49.23, H 3.90, N 15.95; found: C 49.48, H 4.26, N 16.48. IR (KBr pellet): 3420 (sb, water ν O–H), 3261 (m, amide ν N–H), 3076m, 2952 (m, aromatic ν C–H), 1683 (s, amide ν C=O), 1614 (m, amide δ N–H), 1587s, 1550s, 1487s, 1425s, 1384 (s, NO_3^- ν N–O), 1317s, 1296s, 1280w, 1240s, 1193w, 1130w, 1108w, 1064w, 1037w, 935w, 811w, 725m, 698m, 649w cm^{-1}.

4b: yield = 20 mg. Several attempts to solve the single crystal structure of **4b** failed, presumably due to poor quality data. However, the crystal appeared to belong to the centrosymmetric tetragonal *I*4/*m* space group with the following cell parameters: a = 15.465(3), b = 15.465(3), c = 15.377(3) Å, v = 3677.7(12) Å^3. Data collected on several crystals of **4b** resulted in the identical space group and cell parameters. Since these parameters matched well with that of **3** and because the structural model (which failed to refine) obtained from the electron density map of **4b** appeared to be of a metallacryptand type, this suggests that **4b** is probably isostructural with **3**. Based on these findings, we assigned the chemical formula of **4b** as [{Cu(μ-**L1**)$_2$(H$_2$O)$_2$}·(NO$_3$)$_2$]. In addition, the elemental analysis based on this formula matched quite well with the calculated value. Elemental analysis calcd. for $C_{72}H_{64}N_{20}O_{24}Cu_2$ (%): C 50.26, H 3.75, N 16.28; found: C 50.48, H 4.06, N 15.76. IR (KBr pellet): 3309 (m, water ν O–H), 3269 (m, amide ν N–H), 3153w, 3134w, 3070 (m, aromatic ν C–H), 1683 (s, amide ν C=O), 1612 (s, amide δ N–H), 1585m, 1545s, 1489s, 1419s, 1392 (s, NO_3^- ν N–O), 1332s, 1300s, 1234s, 1195s, 1134w, 1111w, 1101w, 1082w, 920w, 827w, 808s, 700s, 651m, 615w, 594w, 532w cm^{-1}.

Single crystal X-ray diffraction

X-Ray single crystal data were collected using Mo-K$_\alpha$ (λ = 0.7107 Å) radiation on a SMART APEX diffractometer equipped with a CCD area detector. Data collection, data reduction and structure solution/refinement were carried out using the software package of SMART APEX. All structures were solved by direct methods and refined in a routine manner. In most cases, non-hydrogen atoms were treated anisotropically. Whenever possible, the hydrogen atoms were located on a difference Fourier map and refined. In other cases, the hydrogen atoms were geometrically fixed.‡

Magnetic measurements

Magnetic measurements were carried out in the Servei de Magnetoquímica (Universitat de Barcelona) on polycrystalline samples (20 mg) with a Quantum Design SQUID MPMS-XL susceptometer working in the 2–300 K range. The magnetic field was 0.1 T. The diamagnetic corrections were evaluated from Pascal's constants. EPR spectra were recorded on powder samples at X-band frequency with a Bruker 300E automatic spectrometer at room temperature.

Acknowledgements

We thank Department of Science & Technology (DST), New Delhi, India for financial support. N. N. A. thanks IACS for research fellowships. Single crystal X-ray diffraction was performed at the DST-funded National Single Crystal Diffractometer Facility at the Department of Inorganic Chemistry, IACS. J. R. acknowledges financial support from the Spanish Government (Grant CTQ2006/03949).

References

1 C. H. Park and H. E. Simmons, *J. Am. Chem. Soc.*, 1968, **90**, 2431–2432.
2 (*a*) J.-M. Lehn, *Acc. Chem. Res.*, 1978, **11**, 49–57; (*b*) J.-M. Lehn and F. Montavon, *Helv. Chim. Acta*, 1978, **61**, 67–82.
3 (*a*) S. O. Kang, M. A. Hossain and K. Bowman-James, *Coord. Chem. Rev.*, 2006, **250**, 3038–3052; (*b*) S. O. Kang, D. Powell, V. W. Day and K. Bowman-James, *Cryst. Growth Des.*, 2007, **7**, 606–608; (*c*) S. O. Kang, V. W. Day and K. Bowman-James, *J. Org. Chem.*, 2010, **75**, 277.
4 (*a*) P. S. Lakshminarayanan, E. Suresh and P. Ghosh, *Angew. Chem., Int. Ed.*, 2006, **45**, 3807–3811; (*b*) P. S. Lakshminarayanan, D. K. Kumar and P. Ghosh, *Inorg. Chem.*, 2005, **44**, 7540–7546; (*c*) I. Ravikumar, P. S. Lakshminarayanan, E. Suresh and P. Ghosh, *Inorg. Chem.*, 2008, **47**, 7992–7999; (*d*) I. Ravikumar, P. S. Lakshminarayanan, E. Suresh and P. Ghosh, *Beilstein J. Org. Chem.*, 2009, **5**, DOI: 10.3762/bjoc.5.41.
5 (*a*) V. McKee, J. Nelson and R. M. Town, *Chem. Soc. Rev.*, 2003, **32**, 309–325; (*b*) J. Nelson, M. Nieuwenhuyzen, I. Pál and R. M. Town, *Dalton Trans.*, 2004, 229–235; (*c*) J. Nelson, M. Nieuwenhuyzen, I. Pál and R. M. Town, *Dalton Trans.*, 2004, 2320–2308; (*d*) M. Arthurs, V. McKee, J. Nelson and R. M. Town, *J. Chem. Educ.*, 2001, **78**, 1269–1272.
6 (*a*) J. L. Dye, *Acc. Chem. Res.*, 2009, **42**, 1564; (*b*) A. Lützen, A. R. Renslo, C. A. Schalley, B. M. O'Leary and J. Rebek, Jr., *J. Am. Chem. Soc.*, 1999, **121**, 7455–7456; (*c*) K. Wichmann, B. Antonioli, T. Söhnel, M. Wenzel, K. Gloe, K. Gloe, J. R. Price, L. F. Lindoy, A. J. Blake and M. Schröder, *Coord. Chem. Rev.*, 2006, **250**, 2987–3003; (*d*) V. Amendola, L. Fabbrizzi, C. Mangano, P. Pallavicini, A. Poggi and A. Taglietti, *Coord. Chem. Rev.*, 2001, **219–221**, 821–837.
7 (*a*) J. W. Steed and J. L. Atwood, *Supramolecular Chemistry*, Wiley, 2nd edn, UK, 2009; (*b*) J. L. Sessler, P. Gale and W.-S. Cho, *Anion Receptor Chemistry*, The Royal Society of Chemistry, Cambridge, UK, 2006; (*c*) J. W. Steed, D. R. Turner and K. Wallace, *Core Concepts in Supramolecular Chemistry and Nanochemistry*, Wiley, England, 2007; (*d*) G. R. Desiraju, *The Crystal as a Supramolecular Entity*, Wiley, Chichester, 1996; (*e*) A. Bianchi, K. Bowman-James and E. García-España, *Supramolecular Chemistry of Anions*, Wiley-VCH, New York, 1997.
8 (*a*) M. Fujita, *Acc. Chem. Res.*, 1999, **32**, 53–61; (*b*) D. B. Amabilino and J. F. Stoddart, *Chem. Rev.*, 1995, **95**, 2725–2828; (*c*) G. Schill, *Catenane, Rotaxanes and Knots*, Academic Press, New York, 1971; (*d*) E. C. Constable and M. D. Ward, *J. Am. Chem. Soc.*, 1990, **112**, 1256–1258; (*e*) D. B. Amabilino, C. O. Dietrich-Buchecker and J.-P. Sauvage, *J. Am. Chem. Soc.*, 1996, **118**, 3285–3286; (*f*) D. Whang and K. Kim, *J. Am. Chem. Soc.*, 1997, **119**, 451–452; (*g*) L. Carlucci, G. Ciani, M. Moret, D. M. Proserpio and S. Rizzato, *Angew. Chem., Int. Ed.*, 2000, **39**, 1506–1510; (*h*) B. F. Hoskins, R. Robson and D. A. Slizys, *Angew. Chem., Int. Ed. Engl.*, 1997, **36**, 2336–2338.
9 (*a*) M. Albrecht, *Chem. Rev.*, 2001, **101**, 3457–3498; (*b*) C. Piguet, G. Bernardinelli and G. Hopfgartner, *Chem. Rev.*, 1997, **97**, 2005–2062; (*c*) B. Hasenknopf, J.-M. Lehn, N. Boumediene,

A. Dupont-Gervais, A. Van Dorsselaer, B. Kneisel and D. Fensker, *J. Am. Chem. Soc.*, 1997, **119**, 10956–10962; (*d*) C. R. Rice, S. Wörl, J. C. Jeffery, R. L Paul and M. D. Ward, *Chem. Commun.*, 2000, 1529–1530; (*e*) M. J. Hannon, C. L. Painting and N. W. Alcock, *Chem. Commun.*, 1999, 2023–2024.

10 (*a*) G. F. Swiegers and T. J. Malefetse, *Chem. Rev.*, 2000, **100**, 3483–3538; (*b*) R. W. Saalfrank, E. Uller, B. Demleitner and I. Bernt, *Struct. Bonding*, 2000, **96**, 149–175; (*c*) D. L. Caulder and K. N. Raymond, *Acc. Chem. Res.*, 1999, **32**, 975–982; (*d*) M. M. Conn and J. Rebek, Jr., *Chem. Rev.*, 1997, **97**, 1647–1668; (*e*) C. J. Jones, *Chem. Soc. Rev.*, 1998, **27**, 289–300; (*f*) M. Fujita, *Chem. Soc. Rev.*, 1998, **27**, 417–425; (*g*) P. Jacopozzi and E. Dalcanale, *Angew. Chem., Int. Ed. Engl.*, 1997, **36**, 613–615; (*h*) M. Albrecht, H. Röttele and P. Burger, *Chem.–Eur. J.*, 1996, **2**, 1264–1268; (*i*) A. K. Bar, R. Chakrabarty, G. Mostafa and P. S. Mukherjee, *Angew. Chem., Int. Ed.*, 2008, **47**, 8455–8459; (*j*) S. R. Seidel and P. J. Stang, *Acc. Chem. Res.*, 2002, **35**, 972–983.

11 (*a*) F. A. Cotton, L. M. Daniels, C. Lin and C. A. Murillo, *J. Am. Chem. Soc.*, 1999, **121**, 4538–4539; (*b*) F. A. Cotton, C. A. Murillo and R. Yu, *Dalton Trans.*, 2006, 3900–3905; (*c*) S.-H. Hwang, C. N. Moorefield, F. R. Fronczek, O. Lukoyanova, L. Echegoyen and G. R. Newkome, *Chem. Commun.*, 2005, 713–715.

12 (*a*) M.-T. Youinou, N. Rahmouni, J. Fischer and J. A. Osborn, *Angew. Chem., Int. Ed. Engl.*, 1992, **31**, 733–735; (*b*) P. J. Stang and D. H. Cao, *J. Am. Chem. Soc.*, 1994, **116**, 4981–4982; (*c*) P. J. Stang and B. Olenyuk, *Angew. Chem., Int. Ed. Engl.*, 1996, **35**, 732–736; (*d*) F. A. Cotton, C. Lin and C. A. Murillo, *J. Am. Chem. Soc.*, 2001, **123**, 2670–2671.

13 (*a*) C. S. Campos-Fernández, R. Clérac, J. M. Koomen, D. H. Russell and K. R. Dunbar, *J. Am. Chem. Soc.*, 2001, **123**, 773–774; (*b*) C. S. Campos-Fernández, B. L. Schottel, H. T. Chifotides, J. K. Bera, J. Bacsa, J. M. Koomen, D. H. Russell and K. R. Dunbar, *J. Am. Chem. Soc.*, 2005, **127**, 12909–12923; (*c*) S.-H. Hwang, P. Wang, C. N. Moorefield, L. A. Godínez, J. Manríquez, E. Bustos and G. R. Newkome, *Chem. Commun.*, 2005, 4672–4674.

14 (*a*) G. R. Newkome, T. J. Cho, C. N. Moorefield, G. R. Baker, R. Cush and P. S. Russo, *Angew. Chem., Int. Ed.*, 1999, **38**, 3717–3721; (*b*) J. R. Hall, S. J. Loeb, G. K. H. Shimizu and G. P. A. Yap, *Angew. Chem., Int. Ed.*, 1998, **37**, 121–123.

15 (*a*) A. P. Davis and R. S. Wareham, *Angew. Chem., Int. Ed.*, 1998, **37**, 2270–2273; (*b*) A. P. Davis and R. S. Wareham, *Angew. Chem., Int. Ed.*, 1999, **38**, 2978–2996; (*c*) G. Lecollinet, A. P. Dominey, T. Velasco and A. P. Davis, *Angew. Chem., Int. Ed.*, 2002, **41**, 4093–4096; (*d*) E. Klein, M. P. Crump and A. P. Davis, *Angew. Chem., Int. Ed.*, 2005, **44**, 298–302; (*e*) S. O. Kang, D. Powell, V. W. Day and K. Bowman-James, *Angew. Chem., Int. Ed.*, 2006, **45**, 1921–1925; (*f*) G. Das, P. Tripathi, A. Tripathi and P. K. Bharadwaj, *Tetrahedron*, 2000, **56**, 1501–1504.

16 D. Krishna Kumar, A. Das and P. Dastidar, *CrystEngComm*, 2007, **9**, 548–555.

17 (*a*) D. Krishna Kumar, A. Das and P. Dastidar, *Cryst. Growth Des.*, 2007, **7**, 2096–2105; (*b*) P. N. W. Baxter, R. G. Khoury, J.-M. Lehn, G. Baum and D. Fenske, *Chem.–Eur. J.*, 2000, **6**, 4140–4148; (*c*) D.-L. Long, A. J. Blake, N. R. Champness, C. Wilson and M. Schröder, *Chem.–Eur. J.*, 2002, **8**, 2026–2033.

18 (*a*) C. Provent, E. Rivara-Minten, S. Hewage, G. Brunner and A. F. Williams, *Chem.–Eur. J.*, 1999, **5**, 3487–3494; (*b*) G. Baum, E. C. Constable, D. Fenske, C. E. Housecroft and T. Kulke, *Chem. Commun.*, 1999, 195–196.

19 (*a*) N. N. Adarsh, D. Krishna Kumar and P. Dastidar, *Inorg. Chem. Commun.*, 2008, **11**, 636–642; (*b*) X.-D. Chen and T. C. W. Mak, *Dalton Trans.*, 2005, 3646–3652; (*c*) A. J. Blake, G. Baum, N. R. Champness, S. S. M. Chung, P. A. Cooke, D. Fenske, A. N. Khlobystov, D. A. Lemenovskii, W.-S. Li and M. Schröder, *J. Chem. Soc., Dalton Trans.*, 2000, 4285–4291; (*d*) M. J. Hannon, C. L. Painting, E. A. Plummer, L. J. Childs and N. W. Alcock, *Chem.–Eur. J.*, 2002, **8**, 2225–2238; (*e*) J. M. Russell, A. D. M. Parker, I. Radosavljevic-Evans, J. A. K. Howard and J. W. Steed, *CrystEngComm*, 2006, **8**, 119–122; (*f*) R. Custelcean, B. A. Moyer, V. S. Bryantsev and B. P. Hay, *Cryst. Growth Des.*, 2006, **6**, 555–563.

20 P. N. W. Baxter, J.-M. Lehn, G. Baum and D. Fenske, *Chem.–Eur. J.*, 2000, **6**, 4510–4517.

21 (*a*) G. Mezei, C. M. Zaleski and V. L. Pecoraro, *Chem. Rev.*, 2007, **107**, 4933–5003; (*b*) Y. Wang, P. Cheng, Y. Song, D.-Z. Liao and S.-P. Yan, *Chem.–Eur. J.*, 2007, **13**, 8131–8138; (*c*) R. W. Saalfrank, H. Maid and A. Scheurer, *Angew. Chem., Int. Ed.*, 2008, **47**, 8794–8824; (*d*) J. Park, S. Hong, D. Moon, M. Park, K. Lee, S. Kang, Y. Zou, R. P. John, G. H. Kim and M. S. Lah, *Inorg. Chem.*, 2007, **46**, 10208–10213; (*e*) H. Chun, *J. Am. Chem. Soc.*, 2008, **130**, 800–801; (*f*) F. Nouar, J. F. Eubank, T. Bousquet, L. Wojtas, M. J. Zaworotko and M. Eddaoudi, *J. Am. Chem. Soc.*, 2008, **130**, 1833–1835; (*g*) D. J. Tranchemontagne, Z. Ni, M. O_Keeffe and O. M. Yaghi, *Angew. Chem., Int. Ed.*, 2008, **47**, 5136–5147; (*h*) D. K. Chand, K. Biradha, M. Kawano, S. Sakamoto, K. Yamaguchi and M. Fujita, *Chem.–Asian J.*, 2006, **1**, 82–90; (*i*) B. Moulton, J. Lu, A. Mondal and M. J. Zaworotko, *Chem. Commun.*, 2001, 863–864; (*j*) N. Takeda, K. Umemoto, K. Yamaguchi and M. Fujita, *Nature*, 1999, **398**, 794–796; (*k*) S. P. Argent, H. Adams, T. Riis-Johannessen, J. C. Jeffery, L. P. Harding, O. Mamula and M. D. Ward, *Inorg. Chem.*, 2006, **45**, 3905–3919; (*l*) B. Olenyuk, J. A. Whiteford, A. Fechtenkotter and P. J. Stang, *Nature*, 1999, **398**, 796–799.

22 (*a*) H. Amouri, L. Mimassi, M. N. Rager, B. E. Mann, C. Guyard-Duhayon and L. Raehm, *Angew. Chem., Int. Ed.*, 2005, **44**, 4543–4546; (*b*) L. J. Barbour, G. W. Orr and J. L. Atwood, *Chem. Commun.*, 2000, 859–860; (*c*) H. Amouri, C. Desmarets, A. Bettoschi, M. N. Rager, K. Boubekeur, P. Rabu and M. Drillon, *Chem.–Eur. J.*, 2007, **13**, 5401–5407; (*d*) P. Diaz, D. M. P. Mingos, R. Vilar, A. J. P. White and D. J. Williams, *Inorg. Chem.*, 2004, **43**, 7597–7604; (*e*) N. L. S. Yue, D. J. Eisler, M. C. Jennings and R. J. Puddephatt, *Inorg. Chem.*, 2004, **43**, 7671–7681; (*f*) C. Daguenet and P. J. Dyson, *Inorg. Chem.*, 2007, **46**, 403–408; (*g*) N. Yue, Z. Qin, M. C. Jennings, D. J. Eisler and R. J. Puddephatt, *Inorg. Chem. Commun.*, 2003, **6**, 1269–1271; (*h*) C.-Y. Su, Y.-P. Cai, C.-L. Chen, H.-X. Zhang and B.-S. Kang, *J. Chem. Soc., Dalton Trans.*, 2001, 359–361; (*i*) L. J. Barbour, G. W. Orr and J. L. Atwood, *Nature*, 1998, **393**, 671–673.

23 (*a*) N. N. Adarsh, D. Krishna Kumar and P. Dastidar, *Cryst. Growth Des.*, 2009, **9**, 2979–2983; (*b*) N. N. Adarsh, D. Krishna Kumar and P. Dastidar, *CrystEngComm*, 2009, **11**, 796–802; (*c*) S. Banerjee, N. N. Adarsh and P. Dastidar, *CrystEngComm*, 2009, **11**, 746–749; (*d*) N. N. Adarsh, D. Krishna Kumar and P. Dastidar, *CrystEngComm*, 2008, **10**, 1565–1573; (*e*) D. Krishna Kumar, A. Das and P. Dastidar, *Cryst. Growth Des.*, 2007, **7**, 205–207; (*f*) D. Krishna Kumar, A. Das and P. Dastidar, *CrystEngComm*, 2007, **9**, 548–555; (*g*) D. Krishna Kumar, A. Das and P. Dastidar, *CrystEngComm*, 2007, **9**, 895–901; (*h*) D. Krishna Kumar, A. Das and P. Dastidar, *Inorg. Chem.*, 2007, **46**, 7351–7361; (*i*) D. Krishna Kumar, A. Das and P. Dastidar, *Cryst. Growth Des.*, 2006, **6**, 1903–1909; (*j*) D. Krishna Kumar, A. Das and P. Dastidar, *CrystEngComm*, 2006, **8**, 805–814; (*k*) D. Krishna Kumar, A. Das and P. Dastidar, *New J. Chem.*, 2006, **30**, 1267–1275; D. Krishna Kumar, A. Das and P. Dastidar, *Inorg. Chem.*, 2005, **44**, 6933–6935.

24 B. Wu, D. Yuan, B. Lou, L. Han, C. Liu, C. Zhang and M. Hong, *Inorg. Chem.*, 2005, **44**, 9175–9184.

25 (*a*) Z. Qin, M. C. Jennings and R. J. Puddephatt, *Chem.–Eur. J.*, 2002, **8**, 735–738; (*b*) Z. Qin, M. C. Jennings and R. J. Puddephatt, *Inorg. Chem.*, 2003, **42**, 1956–1965.

26 (*a*) R. J. Santos-Contreras, F. J. Martínez-Martínez, E. V. García-Báez, I. I. Padilla-Martínez, A. L. Peraza and H. Höpfl, *Acta Crystallogr., Sect. C: Cryst. Struct. Commun.*, 2007, **63**, o239; (*b*) J. E. Gautrot, P. Hodge, D. Cupertino and M. Helliwell, *New J. Chem.*, 2006, **30**, 1801–1807.

27 P. Sluis Van der and A. L. Spek, *Acta Crystallogr., Sect. A: Found. Crystallogr.*, 1990, **46**, 194.

28 R. Custelcean and B. A. Moyer, *Eur. J. Inorg. Chem.*, 2007, 1321–1340.

29 B. F. Hoskins and R. Robson, *J. Am. Chem. Soc.*, 1990, **112**, 1546–1554.

30 (*a*) R. Custelcean and P. Remy, *Cryst. Growth Des.*, 2009, **9**, 1985–1989; (*b*) R. Custelcean, V. Sellin and B. A. Moyer, *Chem. Commun.*, 2007, 1541–1543; (*c*) R. Vilar, *Eur. J. Inorg. Chem.*, 2008, 357–367; (*d*) B. Wu, J. Liang, J. Yang, C. Jia, X.-J. Yang, H. Zhang, N. Tang and C. Janiak, *Chem. Commun.*, 2008, 1762–1764; (*e*) S. Muthu, J. H. K. Yip and J. J. Vittal, *J. Chem.*

Soc., Dalton Trans., 2002, 4561–4568; (*f*) P. Blondeau, A. van der Lee and M. Barboiu, *Inorg. Chem.*, 2005, **44**, 5649–5653; (*g*) V. Amendola, M. Boiocchi, B. Colasson and L. Fabbrizzi, *Inorg. Chem.*, 2006, **45**, 6138–6147; (*h*) C. R. Bondy, P. A. Gale and S. J. Loeb, *J. Am. Chem. Soc.*, 2004, **126**, 5030–5031; (*i*) C.-Y. Su, Y.-P. Cai, C.-L. Chen, H.-X. Zhang and B.-S. Kang, *J. Chem. Soc., Dalton Trans.*, 2001, 359–361; (*j*) B.-C. Tzeng, B.-S. Chen, S.-Y. Lee, W.-H. Liu, G.-H. Lee and S.-M. Peng, *New J. Chem.*, 2005, **29**, 1254–1257.

31 (*a*) C. Thompson, N. R. Champness, A. N. Khlobystov, C. J. Roberts, M. Schröder, S. J. B. Tendler and M. J. Wilkinson, *J. Microsc.*, 2004, **214**, 261–271; (*b*) A. N. Khlobystov, N. R. Champness, C. J. Roberts, S. J. B. Tendler, C. Thompson and M. Schröder, *CrystEngComm*, 2002, **4**, 426–431.

32 (*a*) G. J. Lumetta, The Problem with Anions in the DOE Complex, in *Fundamental and Applications of Anion Separations*, ed. B. A. Moyer and R. P. Singh, Kluwer Academic, New York, 2004, 175–204; (*b*) B. A. Moyer, L. H. Delmau, C. J. Fowler, A. Ruas, D. A. Bostick, J. L. Sessler, E. Katayev, G. D. Pantos, J. M. Llinares, M. A. Hossain, S. O. Kang and K. Bowman-James, Supramolecular Chemistry of Environmentally Relevant Anions, in *Advances in Inorganic Chemistry, vol. 59: Template Effects and Molecular Organization*, ed. R. van. Eldik and K. Bowman-James, Elsevier, Oxford, 2007, pp. 175; (*c*) J. L. Sessler, E. Katayev, G. D. Pantos and Y. A. Ustynyuk, *Chem. Commun.*, 2004, 1276–1277.

33 (*a*) F. Hofmeister, *Naunyn-Schmiedebergs Arch. Pharmacol.*, 1888, **24**, 247; (*b*) W. Kunz, J. Henle and B. W. Ninham, *Curr. Opin. Colloid Interface Sci.*, 2004, **9**, 19.

34 O. Kahn, *Molecular Magnetism*, VCH Publishers, New York, 1993.

35 (*a*) R. Vilar, *Struct. Bonding*, 2008, **129**, 175–206; (*b*) D. K. Chand, K. Biradha, M. Kawano, S. Sakamoto, K. Yamaguchi and M. Fujita, *Chem.–Asian J.*, 2006, **1**, 82–90; (*c*) S. P. Argent, H. Adams, T. Riis-Johannessen, J. C. Jeffery, L. P. Harding, O. Mamula and M. D. Ward, *Inorg. Chem.*, 2006, **45**, 3905–3919; D. Rais, J. Yau, D. M. P. Mingos, R. Vilar, A. J. P. White and D. J. Williams, *Angew. Chem., Int. Ed.*, 2001, **40**, 3464–3467.